N90-21335

PRELIMINARY RESULTS ON 2-DIMENSIONAL INTERFEROMETRY OF HL TAU

Eric V. Tollestrup and Paul M. Harvey
University of Texas at Austin

I. Introduction

Sources with directed outflows occur in a diverse set of objects, including young stellar objects (YSOs), evolved stars, active galactic nuclei, and QSOs. Observations ranging from visible to radio wavelengths show that directed outflows occur over a large range of physical scale lengths and are frequently bipolar. However, most of these observations have not resolved the actual region that produces the directed flow and therefore the mechanism is directly unobserved. But direct observations of the mechanism are needed to study the relationship of directed outflows and nearby physical environment.

What causes the directed outflows? A frequently proposed scenario is to impinge a spherically symmetric stellar outflow onto an asymmetric mass distribution such as a disk or toroid. The asymmetric mass distribution then acts as a funnel or a de Laval nozzle and produces a directed outflow or jet. The biggest observational difficulty is that the asymmetric mass densities occur extremely close to the power source. For example, models by Konigl (*ApJ.***261**, 115, 1982) and Shu, Lizano, and Adams (*Star Forming Regions, Proc of IAU Symp 115*, 417, 1985) for young stellar objects with bipolar flows have the directed flows being produced in the 10 to 10**4 AU range. Generally this resolution can not be achieved for most objects because they are too far away. But one class of objects, nearby (i.e. within 1 kpc) YSOs, are close enough to be imaged on the few 10's of AU scale length with very high resolution techniques. Therefore, nearby YSOs provide a unique opportunity to observe in depth a physical mechanism that could explain many other astrophysically important phenomena.

One very high resolution technique, first proposed by Labyrie (*Astron. Ap.*, **6**, 85, 1970), is speckle interferometry. With speckle interferometry, spatial information down to λ/D is possible, where D is the diameter of the telescope and λ is the wavelength. On a 3-m class telescope this corresponds to 0.11 arcsec at 1.6 μm, 0.15 arcsec at 2.2 μm, and 0.25 arcsec at 3.6 μm. To put this into astrophysical terms, an object in the Taurus dark cloud (150 pc) could be resolved down to 16 AU at H, 22 AU at K, and 37 AU at L'; that is, the size of our solar system and with in the scale size of the above bipolar flow models.

One well known YSO that is a good candidate for studying the relationship between any mass distribution near the star and a directed outflow is HL Tau. It has been studied before with 1-D slit scanning IR speckle interferometry techniques (Beckwith, S., Zuckerman, B., Skrutskie, M. F., and Dyke, H. M., *Ap. J.*, **287**, 793, 1984) and maximum entropy techniques (Grasdalen, G. L., Strom, S. E., Strom, K. M., Capps, R. W., Thompson, D., and Castelez, M., *Ap. J. Letters*, **283**, L57, 1984) and was shown to be extended ~1-2 arcsec in the E-W direction. It also has a strong 3.1 μm ice feature (Cohen, M., *M.N.R.A.S.*, **173**, 279, 1975; Rydgren, A. E., Strom, S. E., and Strom, K. M., *Ap. J. Suppl.*, **30**, 307, 1976) and has optical jets (Mundt, R. and Fried, J. W., *Ap. J. Letter*, **274**, L83, 1983). The extended structure and strong ice feature may be indicative of an asymmetric mass distribution, like those proposed in the above models, which in turn would be the constraining mechanism that creates the optical jet. Motivated by these issues, we have been studying HL Tau and other objects with speckle interferometry using a 2-dimensional IR array camera. In the following sections, we present a small sample of preliminary results obtained for HL Tau.

II. The Observations and Equipment

We have been pursuing sub-arcsecond resolution techniques using the UT IR array camera, which uses a SBRC 58 X 62 InSb array (Orias, G., Hoffman, A. W., and Casselman, M. F., *SPIE*, **627**, 408, 1986) mounted in a Infrared Labs cryogenic dewar (see Figure 1). The camera has standard J, H, K, and L' broad band filters as well as a 2% CVF mounted on a filter wheel. The optics consist of cold field and reimaging lenses for regular imaging plus a warm adjustable negative lens used to obtain the appropriate plate scale for speckle interferometry work. The camera can be run using either LHe or pumped LN2 and the detector temperature can be adjusted by means of a heating resistor. Used in the speckle interferometry mode the average read noise is ~300-450 electrons/pixel.

The observing technique is as follows. We obtain 128 very short integration images (35-300 msec) of an object of interest. This is then repeated for the sky and for a nearby point source. These three steps are repeated many (10 to 30) times, depending on the object's brightness and the seeing quality. The 35-300 msec exposures are required to freeze the seeing, while the point sources are used to measure the point spread function of the atmosphere + telescope + camera. The repetition insures that wildly fluctuating conditions in the sky or instrument will not produce false results and also to improve the S/N ratio for faint objects. To calibrate the plate scale at the detector focal plane, a double star with a well-determined separation is observed using the same technique.

III. Results

We have obtained diffraction limited images on the IRTF 3.0-m, the McDonald Observatory 2.7-m, the AAT 3.9-m, and the UH 2.2-m telescopes. As a demonstration that the 2-dimensional speckle interferometry is working, Figures 2 and 3 show some of the typical data which we have obtained at the McDonald 2.7-m and the AAT 3.9-m telescopes, respectively. In Figure 2, the three left-hand frames show single flat-fielded speckle images (out of a 128 image data cube) while the right-hand side show the corresponding average power spectrum obtained from the whole 128 image data cube. The top image is a ~0.25 arcsec double star, the middle image is a ~0.8 arcsec double star, and the bottom image is a 1.8 arcsec double star. The respective power spectra clearly show the interference-like pattern that a double star will produce in Fourier space. Note that the seeing was excellent; in the top and bottom images each star shows not a speckle pattern but diffraction (i.e. Airy) patterns instead, while in the middle image there is only about six major speckles.

Figure 3 shows similar results; the top three frames show single flat-fielded images (out of a 128 image data cube) while the bottom three frames show the corresponding average power spectra of the whole data cube. The left-hand image is the same 1.8 arcsec double star shown in Figure 2, the middle image is a ~0.2 arcsec double, and the right-hand image is a point source (note the lack of the interfence-like pattern in its power spectrum). Once again the seeing was excellent since the diffraction patterns are clearly seen on the left hand image, the middle image has only one major speckle for each double star component, and the point source shows only three major speckles. Obtaining images with only diffraction patterns or a few major speckles has been fairly common and shows that the seeing improves in the infrared as compared to the visible. It also demonstrates that true diffraction limited imaging in the IR is possible.

As a final demonstration that the technique is working, an autocorrelation and a reconstructed real image of the 1.8 arcsec double star is shown as a contour plot in Figure 4. In Figure 4a a trace through the secondary star shows that it is only two pixels wide and is diffraction limited in the Nyquist sense with 2 sample per resolution size. Figure 4b is a Fienup (*Appl. Opt.*, **21**, 2758, 1982) reconstruction of 4a (rotated by 90 deg) and also shows that both the primary and secondary star are diffraction limited with 2 pixels per resolution size.

Univ. of Texas/McDonald Observatory
Infrared Array Camera

SOLID NITROGEN (50 K)

FIELD LENS

REIMAGING LENS

58 x 62 InSb ARRAY DETECTOR

FILTER WHEEL

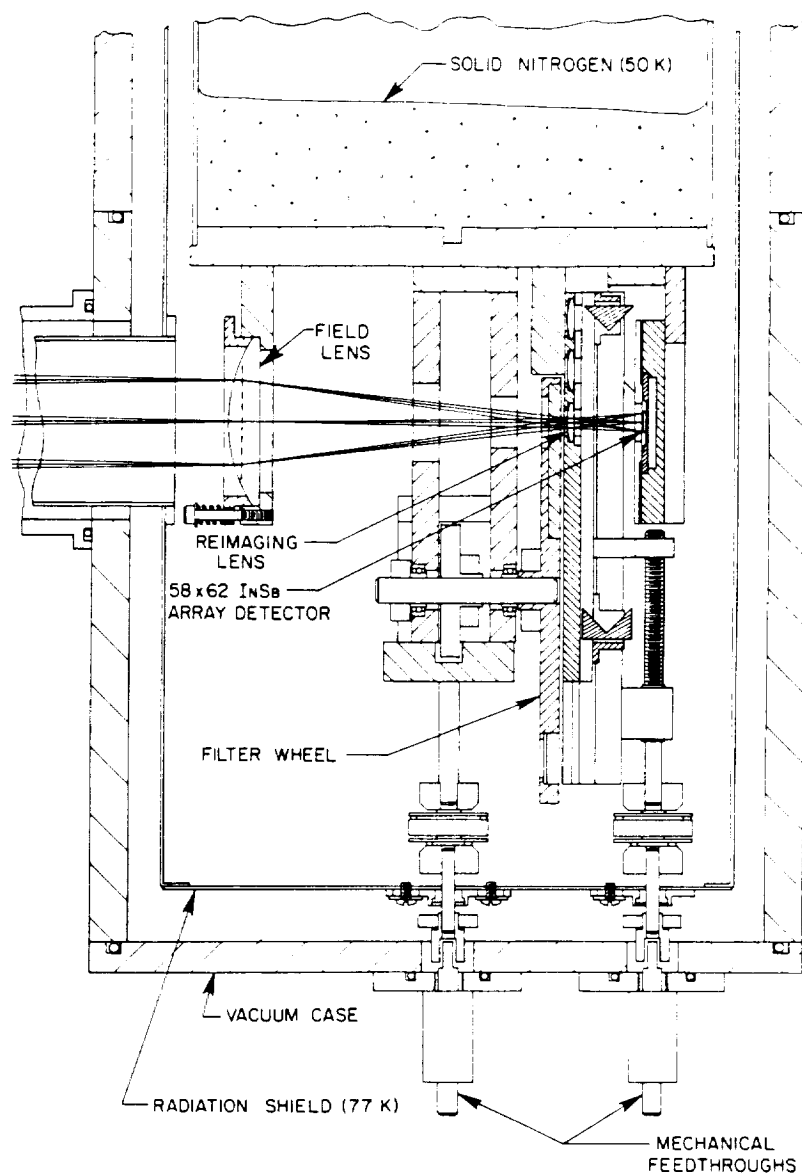VACUUM CASE

RADIATION SHIELD (77 K)

MECHANICAL FEEDTHROUGHS

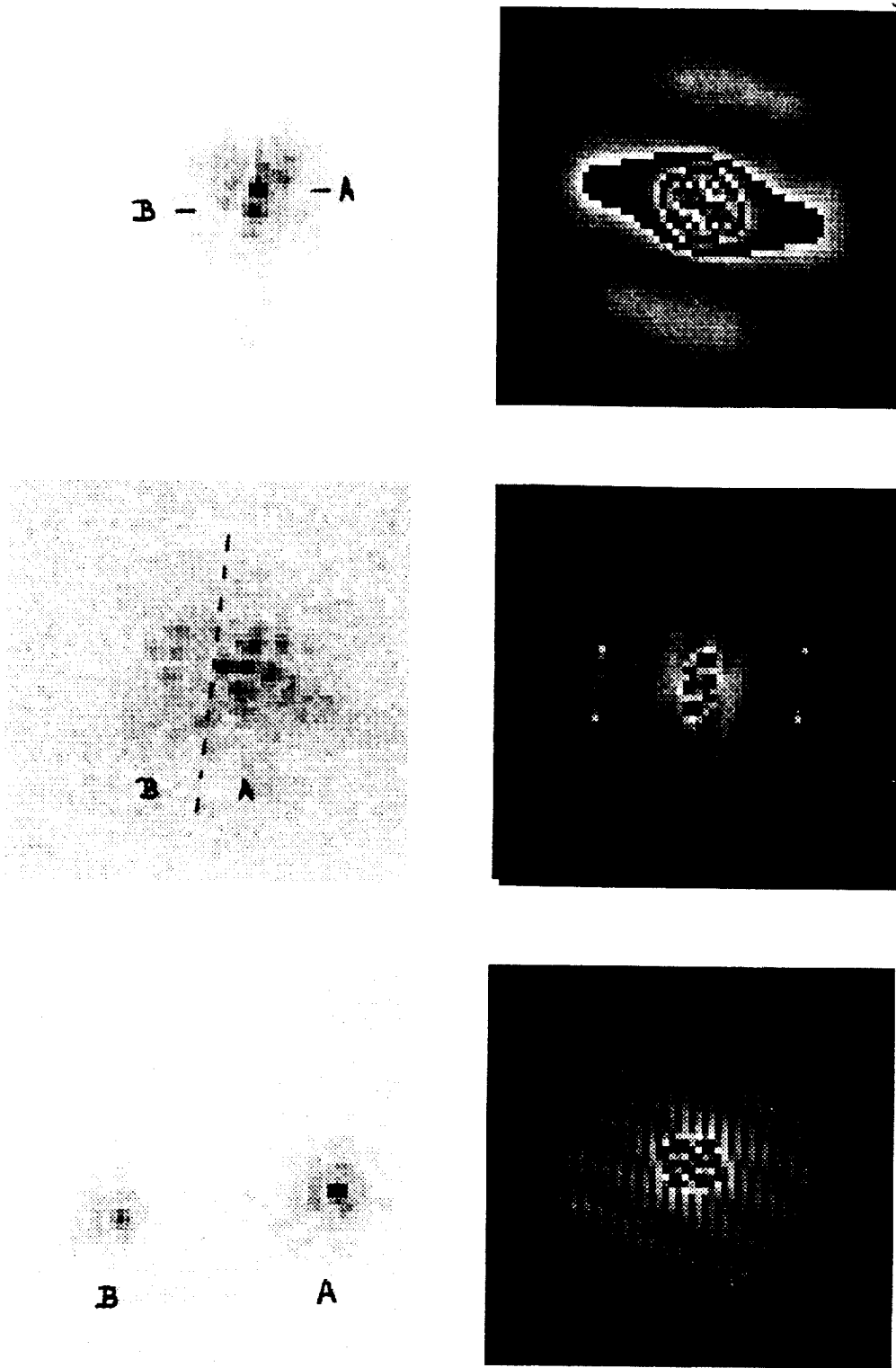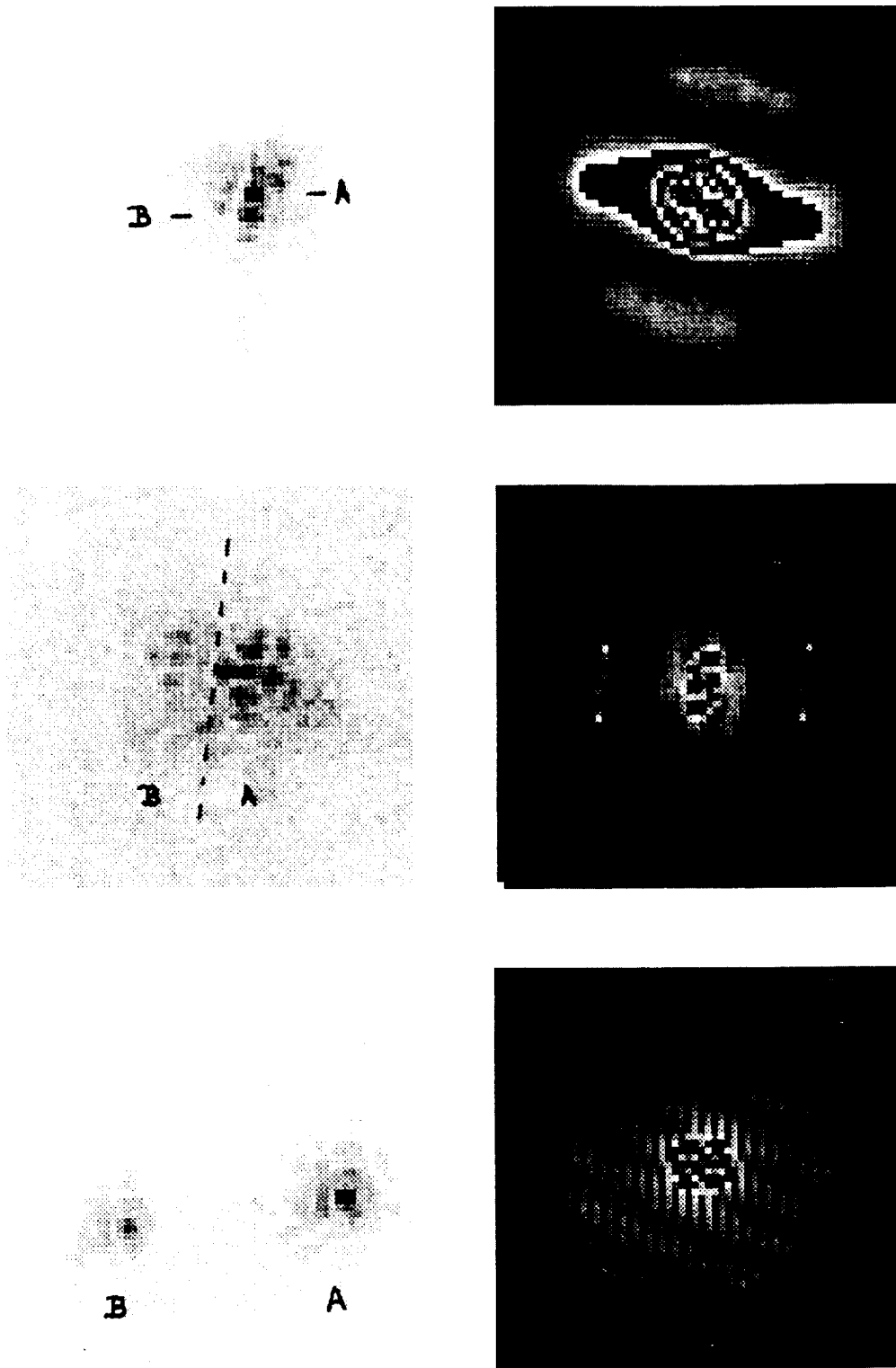Figure 1. Drawing of UT IR array camera deware.

Figure 2. Speckle images (left) and power spectra (right) from McDonald Obs.

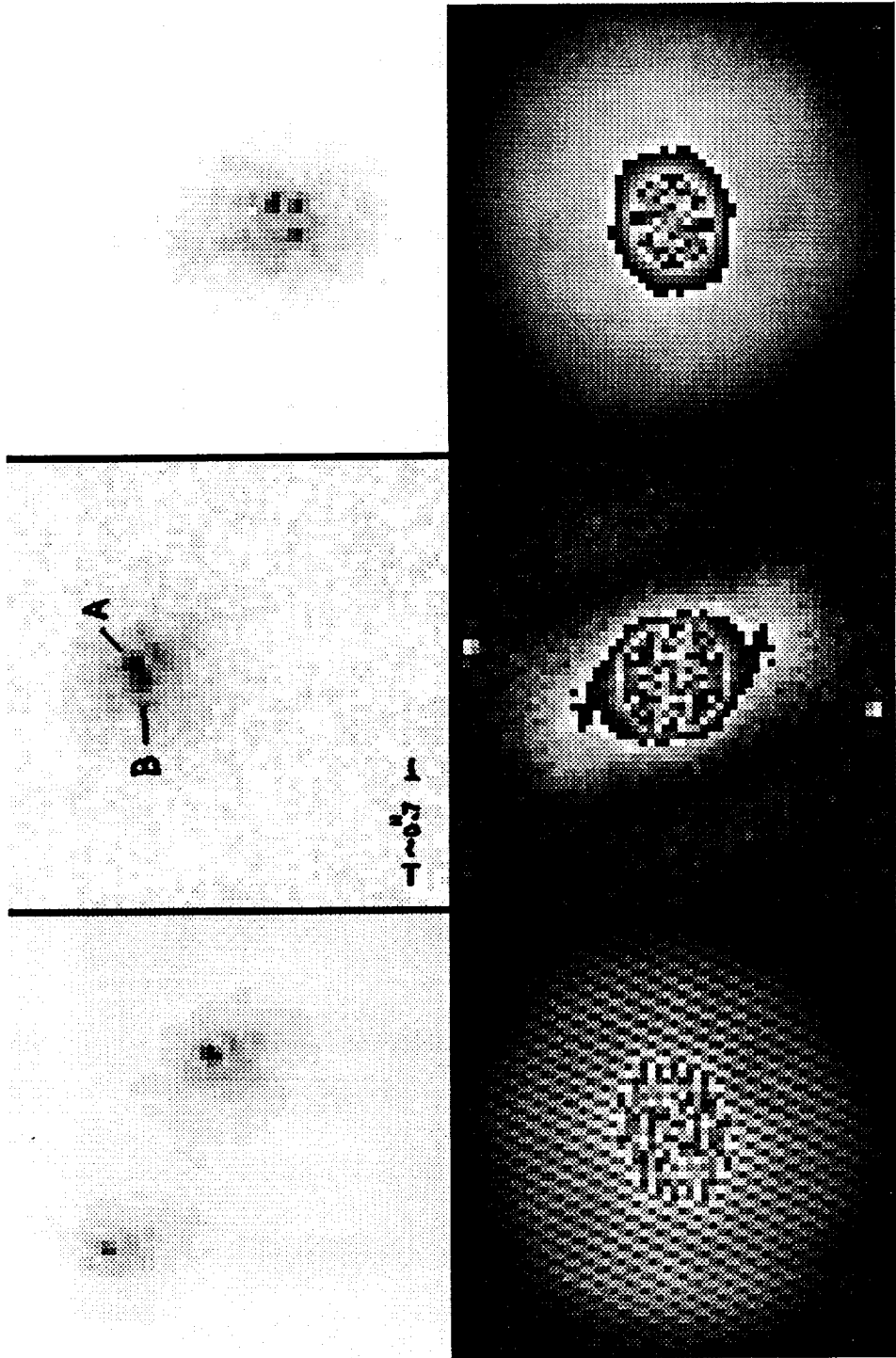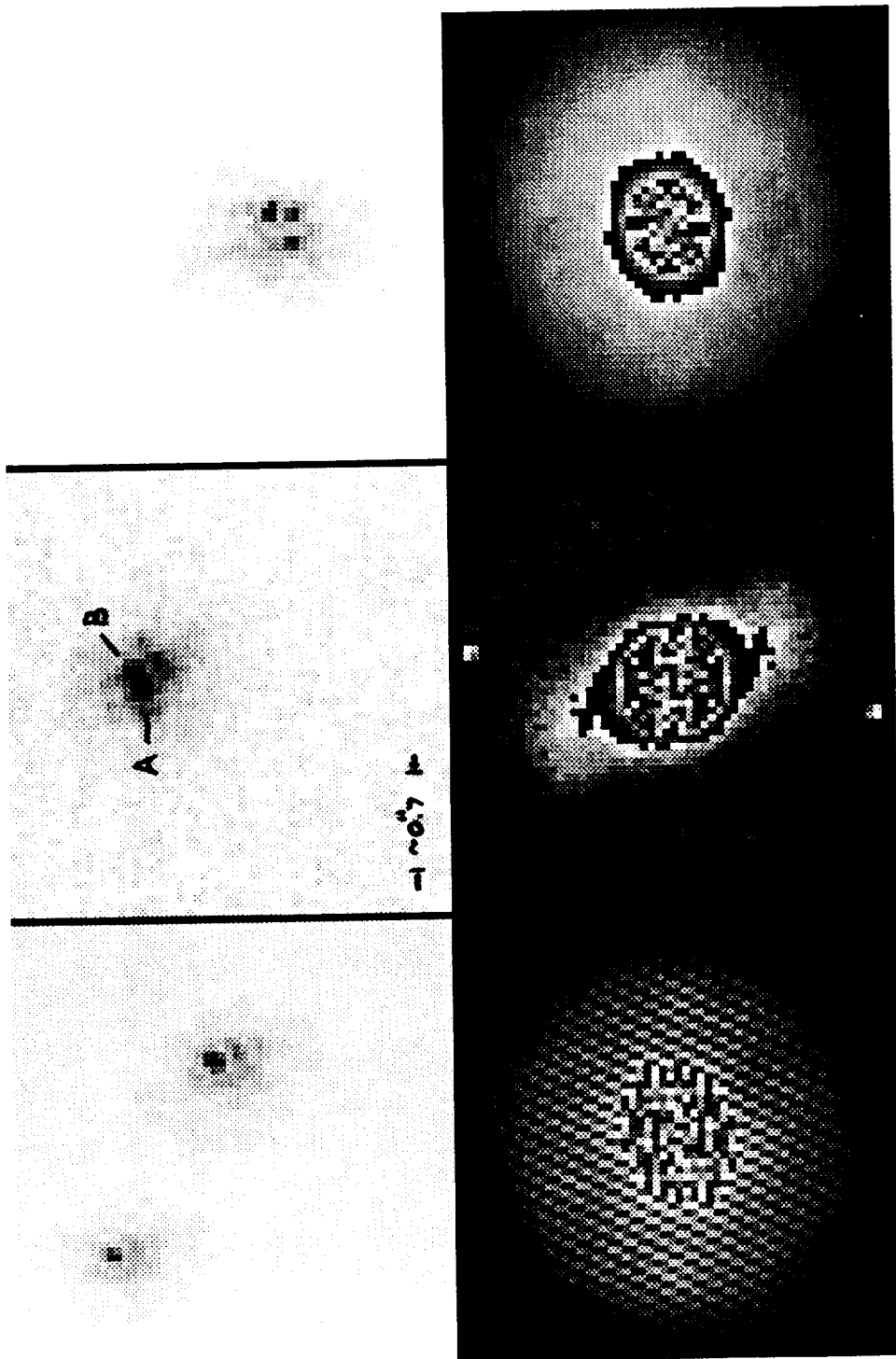Figure 2. Speckle images (left) and power spectra (right) from McDonald Obs.

Figure 3. Speckle images (top) and power spectra (bottom) from AAT.

Figure 3. Speckle images (top) and power spectra (bottom) from AAT.
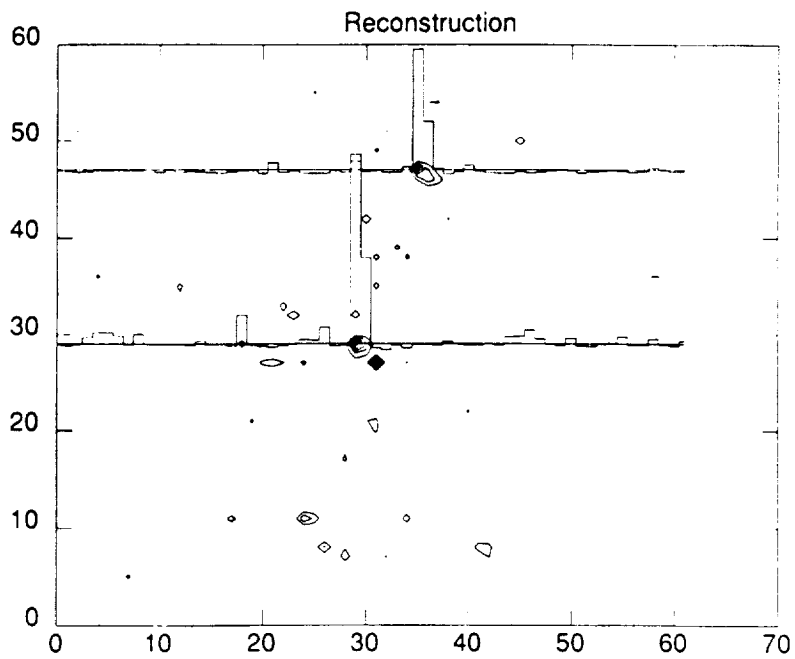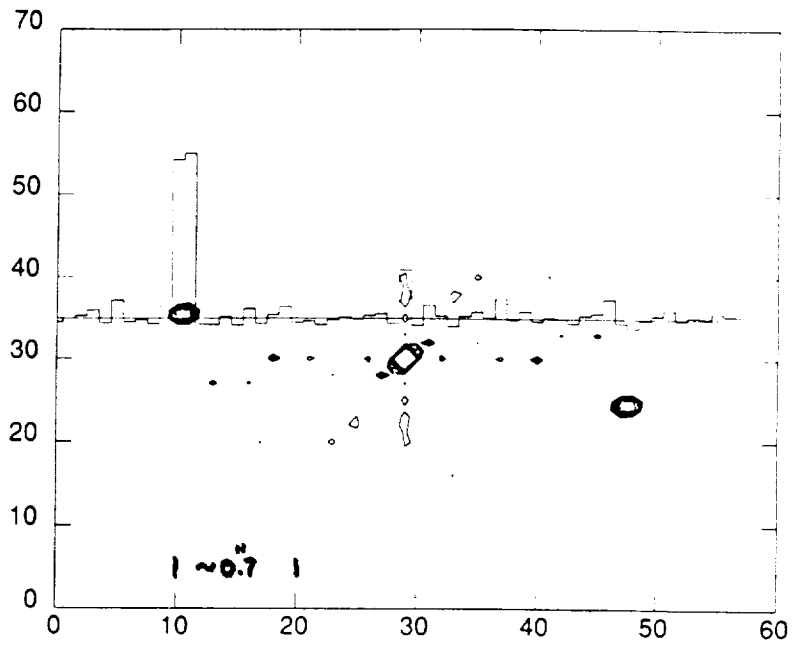
Figure 4. Autocorrelation (a) and Fienup reconstruction (b) of a double star.

IV. HL Tau Results

HL Tau was observed on the McDonald 2.7-m telescope, the IRTF, and the UH 2.2-m telescope in December 1988 and January 1989. Only one night of 2.2µm data from the McDonald run is presented. The data consists of a total of 1792 frames of HL Tau, 1280 frames of the point source SAO 093993 and 1792 frames of the sky. After the average power spectra of HL Tau, the point source, and the sky were calculated, the sky (i.e. noise) power was subtracted from HL Tau and the point source. Then HL Tau was divided by the point source to form the visibility function of HL Tau (see Figure 5). If HL Tau was a point source, then the visibility function would simply be a constant (in this case equal to 1.0) at all spatial frequencies. However, as Figure 5 shows, the visibility functions is not a constant. To get a quantitative examination of the visibility function, a plot of the visibility power versus the magnitude of the spatial frequency is shown in Figure 6 (this is analogous to the visibility functions presented by slit-scanning speckle workers). The telescope cut-off frequency is about 27 units so that the scatter in the data for frequencies above ~27 units is just noise. Two features are evident; the first is the decrease in visibility power from 0 to 10 units, while the second is the flat constant power from 10 to 27 units. The first feature represents a resolved component while the second feature shows that an unresolved component is still present. This is qualitatively the same result that was found by Beckwith *et al* (1984) using slit scanning speckle interferometry. The high frequency noise was filtered and then the visibility function was inverse Fourier transformed to produce an auto-correlation (Figure 7) which shows the unresolved component and the resolved component (Figure 8 shows a blow up of the central 25 X 25 pixel). As Figure 8 shows, the resolved component is about 0.7 arcsec is size. Since this paper is a report on work in progress, a more in depth discussion will be published at a later time.

V. Conclusions

These preliminary 2-dimensional speckle interferometry results of HL Tau are qualitatively similar to those found with 1-dimensional slit scanning techniques; a resolved component (~0.7 arcsec in size) and an unresolved component. We are currently reducing the rest of the data (taken on the three different telescopes and at three different wavelengths) and are also exploring other high resolution methods like the 'shift-and-add' technique and selecting only very best images for processing. The availability of even better 2-dimensional arrays within the next couple of years promises to make speckle interferometry and other high resolution techniques a very powerful and exciting tool for probing a variety of objects in the subarcsec regime.
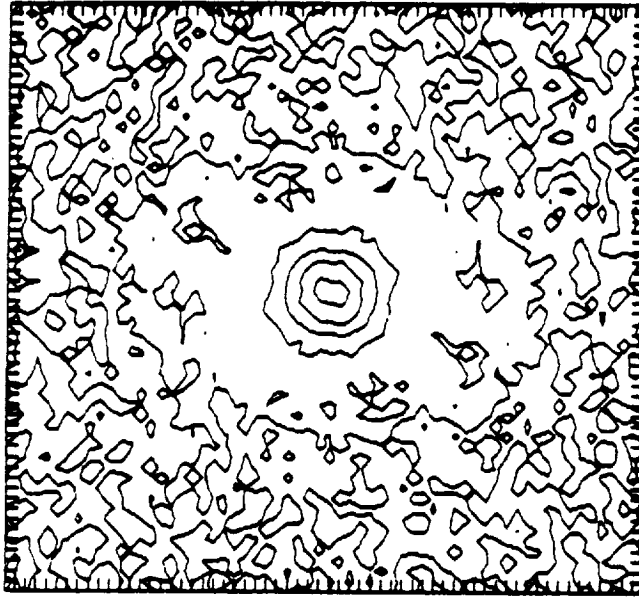
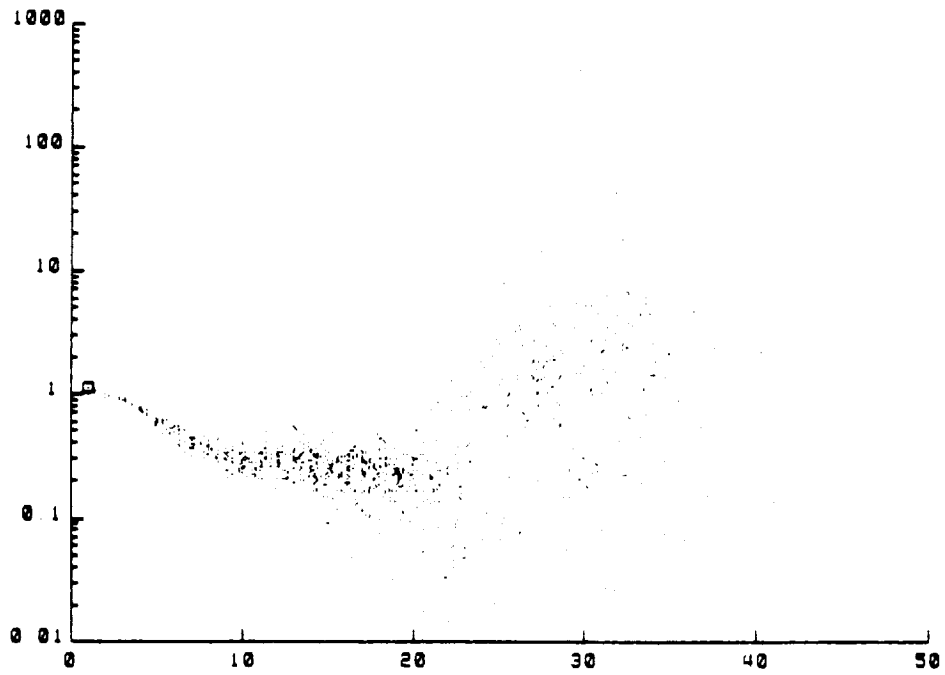Figure 5. 2-D visibility function of HL Tau.

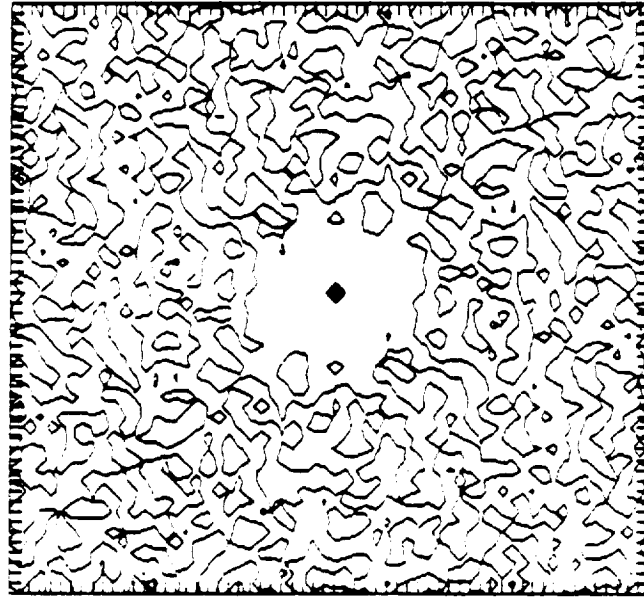Figure 6. Visibility vs magnitude of spatial frequency of HL Tau.

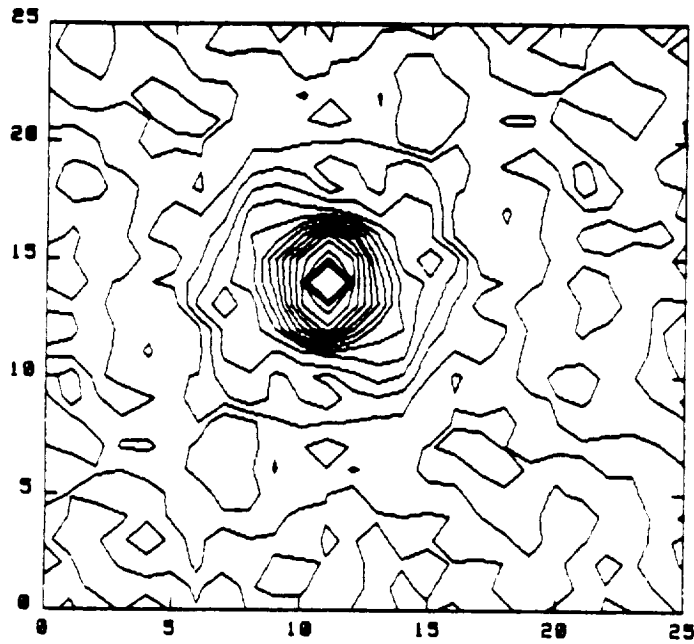Figure 7. Autocorrelation of HL Tau, point spread function removed.

Figure 8. Inner 25 pixels of Figure 7. One pixel is ~0.07 arcsec.